Journal of Applied Fluid Mechanics, Vol. 9, No. 1, pp. 321-331, 2016.
Available online at www.jafmonline.net, ISSN 1735-3572, EISSN 1735-3645.
DOI: 10.18869/acadpub.jafm.68.224.23957

MHD Flow Heat and Mass Transfer of Micropolar Fluid over a Nonlinear Stretching Sheet with Variable Micro Inertia Density, Heat Flux and Chemical Reaction in a Non-darcy Porous Medium

S. Rawat[1], S. Kapoor[2†] and R. Bhargava[3]

[1]*Department of General Studies, Jubail University College, Jubail, Saudi Arabia.*
[2] *Department of Mathematics, Regional Institute of Education, Bhubneswar (NCERT), India*
[3]*Department of Mathematics, Indian Institute of Technology, Roorkee - 247667, India.*

†*Corresponding Author Email: saurabh09.iitr@gmail.com*

(Received July 27, 2014; accepted February 5, 2015)

ABSTRACT

This paper investigates the two dimensional flow, heat and mass transfer of chemically reacting Micropolar fluid over a non-linear stretching sheet with variable heat flux in a non-darcy porous medium. The rate of chemical reaction is assumed to be constant throughout the fluid i.e. homogenous. Using a similarity transformation, the governing partial differential equations are transformed into a system of ordinary differential equation, which is then solved using Finite element method. Numerical results regarding local Nussult No. are shown graphically with Magnetic number (Nm_x) for variation in heat transfer exponent (n). This study also analyzes the effect of velocity exponent m, heat transfer exponent n, material parameter K, Magnetic Number(Nm_x)Darcy NumberDa_x, Forchheimer Number Nf_x, Prandtl number Pr, Schmidt Number Sc and Chemical reaction rate parameter χ_x on velocity, microrotation, temperature and concentration profiles. Velocity exponent m has a positive effect on the velocity, temperature and concentration profiles while microrotation decreases as m increases. Graphical results shows that the thermal boundary layer thickness decreases at and near the wall with the increase in heat flux exponent n. Also an increase in *K* leads to a decrease in skin friction parameter as well as the wall couple stress.

Keywords: Micropolar fluid; MHD; Stretching Sheet; Chemical reaction rate parameter.

1. INTRODUCTION

The stretching sheet problem have been one of the area of great current interest due to its increasing applications in various engineering processes like metal spinning, hot rolling, paper production, extrusions of plastic sheets, continuous casting of metals and spinning of fibres. In all these cases, the quality of the final product depends upon the rate of heat transfer at the stretching surface. Some of the studies illustrating the effects of heat transfer over stretching surface were given by P. Carragher and L.G. Crane[1], T.C. Chiam[2] and R. Cortell[3].Most of the studies mentioned above are dealing with the heat transfer in non-newtonian fluid in the absence of porous medium and magnetic field. But in current scenario, we find a number of industrial applications like magnetohydrodynamic (MHD) accelerators,anti generators, filtration, petroleum reservoirs, Polymer technology and metallurgy[4] etc. where magnetic field is applied to the non–Newtonian fluid in the presence as well as in the absence of porous medium. Ali J. Chamkha[5] studied the flow of an electrically conducting fluid along a vertical plate in a porous medium in the presence of a magnetic field.

One of the important compled fluids analyzed by many authors, is the micropolar fluid,in which the microscopic effects arising from the local structure and micro-motions are also taken into account. Micropolar flow and transport in porous media has received less attention despite important applications in emulsion filtration, polymer gel dynamics in packed beds, petroleum and lubrication industries. The micropolar theory was first introduced by Eringen [6,7] to analyze mathematically the behavior of certain fluid like exotic lubricants, polymers, liquid crystals, animal bloods,real fluids with suspensionsetc., for which the classical Navier–Stokes theory is inadequate.As in the number of chemical engineering operations, it is important to determine to what extent the rate

of mass transfer form a surface to a moving fluid stream will be affected by the presence of chemical reaction, either on the surface itself or in the bulk of the fluid. So the chemical reaction should also be taken into account due to its almost universal occurrence in many branches of science and engineering. Anderson *et al.* [8] studied the diffusion of a chemically reactive species from a stretching sheet. Very recently Beg *et al*.[9] analyzed the double diffusive free convection heat and mass transfer of a chemically reacting micropolar fluid flow over stretching sheet. Rawat et.al [14] introduces the finite element study of natural convection heat and mass transfer in a micropolar fluid-saturated porous regime with soret/dufour effects and hence it used to solve the same technique in [15] Hydromagnetic micropolar free convection heat and mass transfer using darcy-forchheimer porous medium along with thermophysical effects. Bye given a more empasihe one the above problem an attempt has been taken in the direction of linearly stretching sheet, in this study [16] heat and mass transfer phenomena of a Chemically Reacting Micropolar fluid over a linear Stretching Sheet in Darcy Forchheimer Porous Medium, is analysis to explore more the above study a recent attempt [17] has been in taken into account in which two-phase hydromagnetic flow and heat transfer in a particle-suspension through a non-Darcian porous channel using FEM is investigated.

All of the investigations cited above as well as most of the previous existing studies done so far, have considered the microinertia density and heat flux as constant along with that there study is restricted to the linear stretching sheet. So by taking the variable heat flux , variable microinertia density and non darcy porous media in the present study along with non linear stretching sheet, we have tried to analyze a more realistic flow, heat and mass transfer model.

2. MATHEMATICAL ANALYSIS

Here asteady, incompressible, two dimensional flow heat and mass transfer of a chemically reacting micropolarfluid over a stretching sheet with velocity ax^n and variable heat flux$q_w(x) = bx^n$ (where a, b, m and n are constants) in a non-darcy porous medium with a magnetic field B which is applied normal to the surface has been examined . The physical model within coordinate system is presented in Fig (A).

The flow beingconfined to y > 0 where x and y are respectively, the distances along and perpendicular to the surface; u and v are the components of the velocity along x and y directions, respectively. Two equal and opposite forces are introduced along the x-axis so that the wall is stretched keeping the origin fixed. The governing equations for this physical situation are based on the usual balance laws of mass, linear momentum, angular momentum, energy and mass diffusion modified to accountfor the physical effects mentioned above. These equations are given by:

Conservation of Mass:

$$\frac{\partial u}{\partial x} + \frac{\partial v}{\partial y} = 0 \tag{1}$$

Momentum Equation:

$$u\frac{\partial u}{\partial x} + v\frac{\partial v}{\partial y} = \frac{(\mu+\kappa)}{\rho}\frac{\partial^2 u}{\partial y^2} + \frac{\kappa}{\rho}\frac{\partial N}{\partial y} - \frac{\sigma B_0^2}{\rho}u - \frac{(\mu+\kappa)}{\rho k_p}u - b_f u^2 \tag{2}$$

Angular Momentum Equation:

$$\rho j^*\left(u\frac{\partial N}{\partial x} + v\frac{\partial N}{\partial y}\right) = \frac{\partial}{\partial y}\left(\gamma\frac{\partial N}{\partial y}\right) - \kappa(2N + \frac{\partial u}{\partial y}) \tag{3}$$

Conservation of micro-inertia:

$$u\frac{\partial j^*}{\partial x} + v\frac{\partial j^*}{\partial y} = 0 \tag{4}$$

Energy Equation:

$$u\frac{\partial T}{\partial x} + v\frac{\partial T}{\partial y} = \alpha\frac{\partial^2 T}{\partial y^2} \tag{5}$$

Diffusion Equation:

$$u\frac{\partial C}{\partial x} + v\frac{\partial C}{\partial y} = D\frac{\partial^2 C}{\partial y^2} - \Gamma C \tag{6}$$

with boundary conditions defined as:

$$y = 0: \quad u = ax^m, \qquad v = 0\ N = -s(\frac{\partial u}{\partial y}) \qquad j^* = \frac{vx}{(m+1)ax^m},$$

$$\frac{\partial T}{\partial y} = -\frac{q_w}{k}\ , C = C_w \tag{7}$$

$$y \to \infty: u \to 0, N \to 0, T \to T_\infty, C \to C_\infty \tag{8}$$

where , k, j^*, μ are the gyro-viscosity, micro-inertia density and dynamic viscosity of the fluid. s is the surface condition parameter and varies from 0 to 1. N, T, C designate the angular velocity (micro-rotation), temperature and species concentration respectively in the boundary layer. C∞ is the concentration at the free stream, C_w is concentration at the wall (stretching surface), k_p is permeability of the porous medium, $\propto$ is the thermal diffusivity, D is the species diffusivity and Γ is the chemical reaction rate parameter.We had taken $j^*$and γ as functions of the coordinate x and y instead of constants(as in majority of previous studies). In (7) the initial boundary condition for micro-rotation physically corresponds to the *vanishing of the anti-symmetric part of the stress tensor* and corresponds to *weak* concentrations of the micro-elements of the micropolar fluid. The microelement (particle) spin is equal to the fluid vorticity at the boundary for fine particle suspensions. In this scenario therefore the particles are able to sustain rotation in the vicinity of the stretching surface (near-field regime). Following Ahmadi[10] and Gorla[11], we assume that the spin gradient viscosity γ is given by

$\gamma = \left(\mu + \frac{\kappa}{2}\right)j^* = \mu\left(1 + \frac{\kappa}{2}\right)j^*$Using the similarity transformation

$$\eta = \left(\frac{a(m+1)x^{m-1}}{2v}\right)^{1/2} y, \quad u = ax^m f'(\eta),$$

$$v = \left(\left(\frac{a(m+1)v}{2}\right)^{1/2} x^{\frac{m-1}{2}} (f + \frac{(m-1)}{(m+1)}\eta f')\right), \quad N = \left(\frac{a^3(m+1)}{2v}\right)^{1/2} x^{\frac{3m-1}{2}} g(\eta),\ j^* = \frac{2vx}{(m+1)ax^m} I(\eta),$$

$$T = T_\infty + \frac{q_w}{k}\left(\frac{2v}{a(m+1)x^{m-1}}\right)^{1/2} \theta(\eta), \Phi(\eta) = \frac{C-C_\infty}{C_w-C_\infty}, \tag{9}$$

Equations(1)-(6) reduces to the following simultaneous equations:

Momentum Equation:

$$(1+K)f''' + ff'' - \frac{2m}{(m+1)}f'^2 + Kg' - \frac{2}{(m+1)}Nm_x f' - \frac{2(1+K)}{(m+1)Da_x Re_x}f' - \frac{2Nf_x}{(m+1)}f'^2 = 0 \tag{10}$$

Angular Momentum Equation:

$$\left(1+\frac{K}{2}\right)(Ig')' + I\left(fg' - \frac{(3m-1)}{(m+1)}fg'\right) - K(2g + \boldsymbol{f''}) = \mathbf{0} \tag{11}$$

Micro-inertia Equation:

$$2(1-\mathrm{m})\mathrm{f'I} - (\mathrm{m}+1)\mathrm{fI'} = 0 \tag{12}$$

Energy Equation:

$$\theta'' + \mathrm{Prf}\theta' - \frac{(2\mathrm{n}-\mathrm{m}+1)}{(\mathrm{m}+1)}\mathrm{Prf'}\theta \quad = 0 \tag{13}$$

Diffusion Equation:

$$\Phi'' + Scf\Phi' - \frac{2ScRe_x\chi_x}{(m+1)}\Phi = 0 \tag{14}$$

where $K = \frac{\kappa}{\mu}$ is the micropolar parameters(dimensionless material property),$f$is the dimensionless stream function, $\eta$is the dimensionless y-coordinate, Lis the dimensionless micro-inertia density, $\theta$is the dimensionless temperature and Φ is the dimensionless concentration. $Nm_x = \frac{\sigma B_0^2 x}{\rho a x^m}$ is the local magnetic number,$Da_x = \frac{k_p}{x^2}$ is the local darcy number, $Re_x = \frac{ax^m x}{v}$ is the local Reynolds Number,$Nf_x = b_f x$ is the local Forchheimer Number,$Pr = \frac{\vartheta}{\alpha}$is the Prandtl Number,$Sc = \frac{v}{D}$is the Schmidt Number, $\chi_x = \frac{v\Gamma}{a^2x^{2m}}$ is the local dimensionless chemical reaction rate parameter.

With boundary conditions as At

$$\eta = 0:\ f(0) = 0, \quad f'(0) = 1, \quad g(0) = -s(f''0), I(0) = 0.5, \theta'(0) = -1, \Phi(0) = 1 \tag{15}$$

As

$$\eta \to \infty \ \ \frac{df}{d\eta} \to 0\ , g \to 0, \theta \to 0, \Phi \to 0 \tag{16}$$

The shearing stress on the surface is defined as

$$\tau_w = \left[(\mu+\kappa)\frac{du}{dy} + \kappa N\right]_{y=0} = \left(\frac{a^3(m+1)}{2v}\right)^{1/2} x^{\frac{3m-1}{2}}[(\mu + \kappa)f''(0) + kg(0)]$$

In micropolar fluid flow, the physical quantities of principle interest are the skin friction coefficient C_f, the dimensionless wall couple stress, M_w, and the rate of heat transfer so we will be discussing then one by one.

The skin friction coefficient is defined by

$$C_f = \frac{2\tau_w}{\rho(ax^m)^2}$$

The wall couple stress is defined by $M_w = \frac{m_w}{\rho U^2 x}$

The rate of heat transfer from the wall is given by

$$q_w = -k\frac{\partial T}{\partial y}\Big|_{y=0}$$

where k is the coefficient of thermal conductivity.

The local Nussult No. of the heat transfer is defined by

$$Nu_x = \frac{-x\ (\frac{\partial T}{\partial y})_{y=0}}{T_w - T_\infty} = \left(\frac{m+1}{2}\right)^{1/2} \frac{(Re)^{1/2}}{\theta(0)}$$

$$=> \frac{Nu_x}{(Re)^{1/2}} = \left(\frac{m+1}{2}\right)^{1/2} \frac{1}{\theta(0)} \tag{16a}$$

With the aid of equation (9), together with a definition of wall shear stress as

$$\tau_w = \left[(\mu+\kappa)\frac{du}{dy} + \kappa N\right]_{y=0}$$

and the wall couple stress as$m_w = \gamma(\frac{\partial N}{\partial y})_{y=0}$

it can be shown that

$$C_{\ f}Re_x^{1/2} = \sqrt{2(m+1)}\,(1+\frac{K}{2})f''(0)$$

And

$$M_w Re_x = \frac{1}{2}(1+\frac{K}{2})g'(0)$$

$$M_w \mathrm{Re}_x = \frac{1}{2}\left(1+\frac{K}{2}\right)g'(0)\cdot \tag{16b}$$

To solve the differential equation (10-14), with the boundary conditions (15-16), we assume

$$\frac{df}{d\eta} = U \tag{17}$$

The equations (10-14), then get reduced to

$$(1+K)U'' + fU' - \frac{2m}{(m+1)}U^2 + Kg' - \frac{2}{(m+1)}Nm_x U \quad - \frac{2(1+K)}{(m+1)Da_x Re_x}U - \frac{2Nf_x}{(m+1)}U^2 = 0 \tag{18}$$

$$\left(1+\frac{K}{2}\right)(Ig')' + I\left(fg' - \frac{(3m-1)}{(m+1)}Ug\ \right) -$$

$$K(2g + \boldsymbol{U}') = \mathbf{0} \tag{19}$$

$$2(1-m)UI - (m+1)fI' = 0 \tag{20}$$

$$\theta'' + Prf\theta' - \frac{(2n-m+1)}{(m+1)}PrU\theta \quad = 0 \tag{21}$$

$$\Phi'' + Scf\Phi' - \frac{2ScRe_x\chi_x}{(m+1)}\Phi = 0 \tag{22}$$

With the corresponding boundary conditions

At

$\eta = 0: f(0) = 0, U(0) = 1, g(0) = -sf''(0), I(0) = 0.5, \theta'(0) = -1, \Phi(0) = 1$

As $\eta \to \infty \;\; U \to 0\,, g \to 0, \theta \to 0, \Phi \to 0$

For the computational purpose and without loss of generality, ∞ has been fixed as 8. The whole domain is divided into a set of 82 line elements of equal width, each element being two noded.

3. VARIATIONAL FORMULATION

The variational form associated with equations (17)-(22) over a typical two noded linear element (η_e, η_{e+1})

$$\int_{\eta_e}^{\eta_{e+1}} \mathrm{w}_1(\mathrm{f}' - \mathrm{U})\mathrm{d}\eta = 0 \tag{25}$$

$$\int_{\eta_e}^{\eta_{e+1}} \mathrm{w}_2 \left((1+K)U'' + fU' - \frac{2m}{(m+1)}U^2 + Kg' - \frac{2}{(m+1)}Nm_xU - \frac{2(1+K)}{(m+1)Da_xRe_x}U - \frac{2Nf_x}{(m+1)}U^2 \right)\mathrm{d}\eta = 0 \tag{26}$$

$$\int_{\eta_e}^{\eta_{e+1}} \mathrm{w}_3 \left(\left(1+\frac{K}{2}\right)(Ig')' + I\left(fg' - \frac{(3m-1)}{(m+1)}Ug \right) - K(2g + \boldsymbol{U}') \right)\mathrm{d}\eta = 0 \tag{27}$$

$$\int_{\eta_e}^{\eta_{e+1}} \mathrm{w}_4(2(1-m)UI - (m+1)fI')\mathrm{d}\eta = 0 \tag{28}$$

$$\int_{\eta_e}^{\eta_{e+1}} \mathrm{w}_5(\theta'' + Prf\theta' - \frac{(2n-m+1)}{(m+1)}PrU\theta \;\;)\mathrm{d}\eta = 0 \tag{29}$$

$$\int_{\eta_e}^{\eta_{e+1}} \mathrm{w}_6(\Phi'' + Scf\Phi' - \frac{2ScRe_x\chi_x}{(m+1)}\Phi)\mathrm{d}\eta = 0 \tag{30}$$

where $\mathrm{w}_1, \mathrm{w}_2, \mathrm{w}_3, \mathrm{w}_4, \mathrm{w}_5$ and w_6 are arbitrary test functions and may be viewed as the variation in $f, U, g, I, \theta, and\ \Phi$ respectively.

Finite element formulation:

The finite element model may be obtained from equations (25)-(30) by substituting finite element approximations of the form

$$f = \sum_{j-1}^{2} f_j\psi_j \;\;, U = \sum_{j-1}^{2} U_j\psi_j \;\;, g = \sum_{j-1}^{2} g_j\psi_j$$
$$I = \sum_{j-1}^{2} I_j\psi_j \;\;, \theta = \sum_{j-1}^{2} \theta_j\psi_j \;\;, \Phi = \sum_{j-1}^{2} \Phi_j\psi_j \tag{20}$$

With

$$\mathrm{w}_1 = \mathrm{w}_2 = \mathrm{w}_3 = \mathrm{w}_4 = \mathrm{w}_5 = \mathrm{w}_6 = \psi_i \qquad \mathrm{i}=1,2 \tag{23}$$

where ψ_i are the shape functions for a typical element $(\eta_e, \eta_{e+1})$and are taken as

$$\Psi_1^{(e)} = \frac{\eta_{e+1} - \eta}{\eta_{e+1} - \eta_e}\,, \Psi_2^{(e)} = \frac{\eta - \eta_e}{\eta_{e+1} - \eta_e}\eta_e, \leq \eta \leq \eta_{e+1} \tag{24}$$

The finite element model of the equations thus formed is given by

$$\begin{bmatrix} [K^{11}] & [K^{12}] & [K^{13}][K^{14}] & [K^{15}] & [K^{16}] \\ [K^{21}] & [K^{22}] & [K^{23}][K^{24}] & [K^{25}] & [K^{26}] \\ [K^{31}] & [K^{32}] & [K^{33}][K^{34}] & [K^{35}] & [K^{36}] \\ [K^{41}] & [K^{42}] & [K^{43}][K^{44}] & [K^{45}] & [K^{46}] \\ [K^{51}] & [K^{52}] & [K^{53}][K^{54}] & [K^{55}] & [K^{56}] \\ [K^{61}] & [K^{62}] & [K^{63}][K^{64}] & [K^{65}] & [K^{66}] \end{bmatrix} \begin{bmatrix} \{f\} \\ \{U\} \\ \{g\} \\ \{I\} \\ \{\theta\} \\ \{\Phi\} \end{bmatrix} = \begin{bmatrix} \{b^1\} \\ \{b^2\} \\ \{b^3\} \\ \{b^4\} \\ \{b^5\} \\ \{b^6\} \end{bmatrix} \tag{31}$$

where $[K^{mn}]$ and $[b^m]$ (m.n=1,2,3,4,5,6)are the matrices of order 2 x 2 and 2 x 1 respectively. All these matrices may be defined as follows

$$K_{ij}^{11} = -\int_{\eta_e}^{\eta_{e+1}} \psi_i \frac{d\psi_j}{d\eta}d\eta\,, \qquad K_{ij}^{12} = -\int_{\eta_e}^{\eta_{e+1}} \psi_i\psi_j d\eta$$

$$K_{ij}^{13} = K_{ij}^{14} = K_{ij}^{15} = K_{ij}^{16} = 0 \;\; , K_{ij}^{21} = 0,$$

$$K_{ij}^{22} = -(1+K)\int_{\eta_e}^{\eta_{e+1}} \frac{d\psi_i}{d\eta}\frac{d\psi_j}{d\eta}d\eta + \overline{f_1}\int_{\eta_e}^{\eta_{e+1}} \psi_i\psi_1\frac{d\psi_j}{d\eta}d\eta + \overline{f_2}\int_{\eta_e}^{\eta_{e+1}} \psi_i\psi_2\frac{d\psi_j}{d\eta}d\eta - \frac{2m}{(m+1)}\left(\overline{U_1} + \overline{U_2}\int_{\eta_e}^{\eta_{e+1}} \psi_i\psi_2\psi_j d\eta\right) - \frac{2Nm_x}{(m+1)}\int_{\eta_e}^{\eta_{e+1}} \psi_i\psi_j d\eta$$

$$-\frac{2(K+1)}{(m+1)\boldsymbol{Da_x Re_x}}\int_{\eta_e}^{\eta_{e+1}}\psi_i\psi_j d\eta - \frac{\boldsymbol{2Nf_x}}{(\boldsymbol{m+1})}\left(\overline{U_1}\int_{\eta_e}^{\eta_{e+1}}\psi_i\psi_1\psi_j d\eta + \overline{U_2}\int_{\eta_e}^{\eta_{e+1}}\psi_i\psi_2\psi_j d\eta\right)=0$$

$$K_{ij}^{23}=K\int_{\eta_e}^{\eta_{e+1}}\psi_i\frac{d\psi_j}{d\eta}d\eta$$

$$K_{ij}^{24}=K_{ij}^{25}=K_{ij}^{26}=0\quad,\quad K_{ij}^{31}=0,$$

$$K_{ij}^{32}=-K\int_{\eta_e}^{\eta_{e+1}}\psi_i\frac{d\psi_j}{d\eta}d\eta$$

$$\begin{aligned}K_{ij}^{33}&=\left(1+\frac{K}{2}\right)\overline{I_1}\int_{\eta_e}^{\eta_{e+1}}\psi_i\frac{d\psi_1}{d\eta}\frac{d\psi_j}{d\eta}d\eta\\&+\left(1+\frac{K}{2}\right)\overline{I_2}\int_{\eta_e}^{\eta_{e+1}}\psi_i\frac{d\psi_2}{d\eta}\frac{d\psi_j}{d\eta}d\eta\\&-\left(1+\frac{K}{2}\right)\overline{I_1}\left(\int_{\eta_e}^{\eta_{e+1}}\psi_1\frac{d\psi_i}{d\eta}\frac{d\psi_j}{d\eta}d\eta+\int_{\eta_e}^{\eta_{e+1}}\psi_i\frac{d\psi_1}{d\eta}\frac{d\psi_j}{d\eta}d\eta\right)\\&-\left(1+\frac{K}{2}\right)\overline{I_2}\left(\int_{\eta_e}^{\eta_{e+1}}\psi_2\frac{d\psi_i}{d\eta}\frac{d\psi_j}{d\eta}d\eta+\int_{\eta_e}^{\eta_{e+1}}\psi_i\frac{d\psi_2}{d\eta}\frac{d\psi_j}{d\eta}d\eta\right)+\overline{f_1}\overline{I_1}\int_{\eta_e}^{\eta_{e+1}}\psi_i\psi_1^2\quad\frac{d\psi_j}{d\eta}d\eta\\&+\overline{f_1}\overline{I_2}\int_{\eta_e}^{\eta_{e+1}}\psi_i\psi_1\psi_2\quad\frac{d\psi_j}{d\eta}d\eta+\overline{f_2}\overline{I_1}\int_{\eta_e}^{\eta_{e+1}}\psi_i\psi_1\psi_2\quad\frac{d\psi_j}{d\eta}d\eta\\&+\overline{f_2}\overline{I_2}\int_{\eta_e}^{\eta_{e+1}}\psi_i\psi_2^2\quad\frac{d\psi_j}{d\eta}d\eta\\&-\frac{(3m-1)}{(m+1)}(\overline{U_1}\overline{I_1}\int_{\eta_e}^{\eta_{e+1}}\psi_i\psi_1^2\psi_j\quad d\eta\\&+\overline{U_1}\overline{I_2}\int_{\eta_e}^{\eta_{e+1}}\psi_i\psi_1\psi_2\quad\psi_j d\eta)\\&-\frac{(3m-1)}{(m+1)}(\overline{U_2}\overline{I_2}\int_{\eta_e}^{\eta_{e+1}}\psi_i\psi_2^2\psi_j\quad d\eta\\&+\overline{U_2}\overline{I_1}\int_{\eta_e}^{\eta_{e+1}}\psi_i\psi_1\psi_2\quad\psi_j d\eta)-2K\int_{\eta_e}^{\eta_{e+1}}\psi_i\psi_j d\eta\end{aligned}$$

$$K_{ij}^{34}=K_{ij}^{35}=K_{ij}^{36}=0\quad,K_{ij}^{41}=K_{ij}^{42}=K_{ij}^{43}=0$$

$$\begin{aligned}K_{ij}^{44}&=2(1-m)\overline{U_1}\int_{\eta_e}^{\eta_{e+1}}\psi_i\psi_1\psi_j d\eta\\&+2(1-m)\overline{U_2}\int_{\eta_e}^{\eta_{e+1}}\psi_i\psi_2\psi_j d\eta\\&-(1+m)\overline{f_1}\int_{\eta_e}^{\eta_{e+1}}\psi_i\psi_1\frac{d\psi_j}{d\eta}d\eta\\&-(1+m)\overline{f_2}\int_{\eta_e}^{\eta_{e+1}}\psi_i\psi_2\frac{d\psi_j}{d\eta}d\eta\end{aligned}$$

$$K_{ij}^{45}=K_{ij}^{46}=0\,,K_{ij}^{51}=K_{ij}^{52}=K_{ij}^{53}=K_{ij}^{54}=0$$

$$\begin{aligned}K_{ij}^{55}&=-\int_{\eta_e}^{\eta_{e+1}}\frac{d\psi_i}{d\eta}\frac{d\psi_j}{d\eta}d\eta\\&+\quad Pr\,\overline{f_1}\int_{\eta_e}^{\eta_{e+1}}\psi_i\psi_1\frac{d\psi_j}{d\eta}d\eta\\&+Pr\overline{f_2}\int_{\eta_e}^{\eta_{e+1}}\psi_i\psi_2\frac{d\psi_j}{d\eta}d\eta\\&-\frac{(2m-m+1)}{(m+1)}\left(Pr\overline{U_1}\int_{\eta_e}^{\eta_{e+1}}\psi_i\psi_1\psi_j d\eta+Pr\overline{U_2}\int_{\eta_e}^{\eta_{e+1}}\psi_i\psi_2\psi_j d\eta\right),\end{aligned}$$

$$K_{ij}^{56}=0\,,K_{ij}^{61}=K_{ij}^{62}=K_{ij}^{63}=K_{ij}^{64}=K_{ij}^{65}=0\,,$$

$$\begin{aligned}K_{ij}^{66}=&-\int_{\eta_e}^{\eta_{e+1}}\frac{d\psi_i}{d\eta}\frac{d\psi_j}{d\eta}d\eta\\&+\quad Sc\,\overline{f_1}\int_{\eta_e}^{\eta_{e+1}}\psi_i\psi_1\frac{d\psi_j}{d\eta}d\eta\\&+Sc\overline{f_2}\int_{\eta_e}^{\eta_{e+1}}\psi_i\psi_2\frac{d\psi_j}{d\eta}d\eta\\&-\frac{2ScRe_x\chi_x}{(m+1)}\int_{\eta_e}^{\eta_{e+1}}\psi_i\psi_j d\eta\end{aligned}$$

$$b_i^1=0\,,b_i^2=-(1+K)\left(\psi_i\frac{\mathrm{dU}}{d\eta}\right)_{\eta_e}^{\eta_{e+1}}\,,$$

$$b_i^3=-\left(1+\tfrac{K}{2}\right)\overline{I_1}\left(\psi_i\psi_1\frac{dg}{d\eta}\right)_{\eta_e}^{\eta_{e+1}}-\left(1+\tfrac{K}{2}\right)\overline{I_2}\left(\psi_i\psi_2\frac{dg}{d\eta}\right)_{\eta_e}^{\eta_{e+1}},$$

$$b_i^4=0\quad,\quad b_i^5=-\left(\psi_i\frac{d\theta}{d\eta}\right)_{\eta_e}^{\eta_{e+1}}\quad,\quad b_i^6=-\left(\psi_i\frac{d\Phi}{d\eta}\right)_{\eta_e}^{\eta_{e+1}}$$

Where $\bar{f}=\sum_{i=1}^{2}\overline{f_i}\psi_i$, $\overline{U}=\sum_{i=1}^{2}\overline{U_i}\psi_i$

$$\bar{I} = \sum_{i=1}^{2} \bar{I}_i \psi_i$$

Each element matrix is of the order 12 x 12. The whole domain is divided into a set of 82 line elements. Thus after assembly of all the elements equations, we obtain a matrix of order 498 x 498. This system of equations is non-linear therefore an iterative scheme has been used to solve it. The system is linearized by incorporating the functions $\bar{f}, \bar{U}$ *and* $, \bar{I}$ which are assumed to be known. After applying the given boundary conditions only a system of 488 equations are left which has been solved using iterative method by maintaining an accuracy of 0.0005

Results and Discussion

The set of differential equations (25)-(30) with boundary conditions (23)-(24) has been solved numerically using FEM, taking default parameter as s = 0.5, m = 2.0,n = 1.0, Nm_x= 1.0, Da_x= 1.0, Nf_x= 2.0, Re_x =4.0, K= 1.0, Pr= 0.7, Sc= 0.2 , χ = 1.0, unless otherwise indicated. In order to assess the accuracy of our method, we have compared our local Nusselt No.$\frac{Nu_x}{Re_x^{1/2}}$with that of Elbashbeshy [12]. In both the cases our results are found to be in good agreement and are demonstrated by Table 1. Comparisions have also been made with the Finite difference method(details of which are not given for brevity) and results are shown in the Table 2. Excellent correlation is observed between both methods for dimensional velocity and temperature profile.

Table 1 Values of local Nusselt Number $Nu_x / \mathrm{Re}_x^{1/2}$ for various values of m, n for Newtonian fluid (when terms containing K and I are absent and $Da_x = \infty$, $Fs_x = Nm_x = Sc = 0$)

m	n	Pr=1	Pr=10	Pr=1	Pr=10
-0.2	0.0	0.81990	2.79970	0.8189	2.8008
	1.0	1.2606	4.188	1.2604	4.1881
1.0	0.0	0.58210	2.30730	0.5822	2.3074
	1.0	1.0	3.7202	1.0000	3.7206
5.0	0.0	0.3670	1.6191	0.3668	1.6195
	1.0	0.6849	2.8857	0.6849	2.8857

Fig. 1 shows the variation of the local Nusselt Number with local Magnetic Number $Nm_x$with the variation of heat flux exponent n, keeping all other parameter fixed. It is observed that heat transfer at the surface of the plate increases with the increase in heat flux exponent n as well as Magnetic number.

Figs. 2-5 have been plotted to show the effect of velocity exponent m on velocity, microrotation, temperature and concentration profiles. As expected, the velocity, temperature and concentration profiles increase with the increase in velocity exponent m which is graphically demonstrated by Figs 2,4 and 5.

Table 2 Comparison of Finite Difference and Finite Element Computations
s = 0.5, m = 2, n = 1.0, Re = 4.0, Nm_x= 1.0, Da_x= 1.0, Nf_x= 2.0, K = 1.0, Pr = 0.7, Sc = 0.2, χ = 1.0

	U		θ	
η	FEM	FDM	FEM	FDM
0	1	1	1.84229	1.84226
0.682927	0.405792	0.40581	1.23246	1.23241
1.36585	0.166762	0.16675	0.803489	0.803473
2.04878	0.068237	0.068215	0.510985	0.510976
2.73171	0.027611	0.027605	0.317622	0.317620
3.41463	0.011007	0.011002	0.192482	0.192479
4	0.004933	0.004932	0.122829	0.122828
4.58537	0.002175	0.002172	0.076789	0.076787
5.26829	0.000815	0.000807	0.04311	0.043102
5.95122	0.000292	0.000283	0.023062	0.023054
6.63415	9.61E-05	8.21E-05	0.011354	0.011342
7.31707	2.43E-05	1.12E-05	0.004376	0.004351
8	0	0	0	0

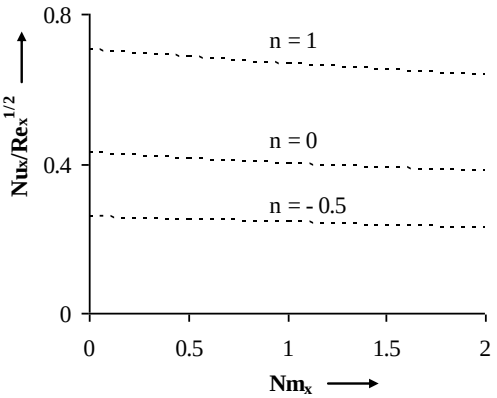

Fig. 1. Variation of the local Nusselt Number $Nu_x / \mathrm{Re}_x^{1/2}$ with K for various values of n.

Fig. 4 also enlightens the fact that velocity exponent m could be one of the key parameters to regulate the temperature, as required in many industrial applications. In Fig. 2, it is observed that initially microrotation, g, decreases as m increases. We may infer that close to the wall, micro-rotation is inhibited as the particles have difficulty in rotating due to the presence of the

wall.Howeverfor the remainder of the domain, microrotation g, increases with the increase in velocity exponent m.

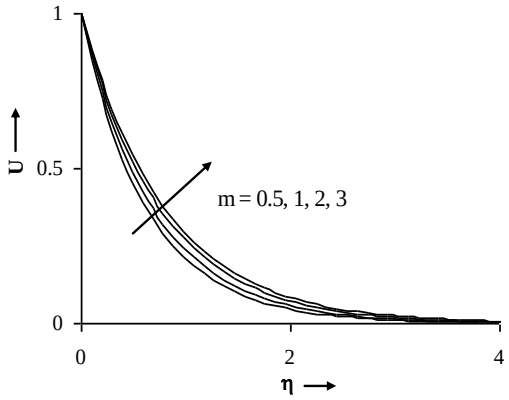

Fig. 2. Effect of velocity exponent m on velocity U

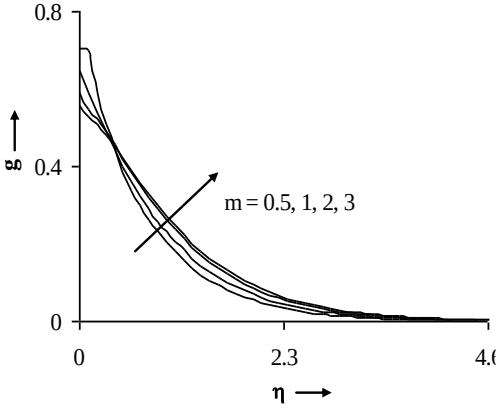

Fig. 3: Effects of velocity exponent m on microrotation g.

Fig 6. illustrates that, the thermal boundary layer thickness decreases with the increase in heat tranfer exponent n.Also the surface temperature decreases with the increase in heat exponent n. This fact is well in agreement with the variation of the local Nusselt number presented in Fig. 1 for fixed values of other parameters.

Figs. 7-8 present the velocity and temperature profiles for different values of Magnetic number Nm_x. It is a well known fact that the application of uniform magnetic field normal to the flow direction gives rise to a forcecalled Lorentz force. Thisforce has a tendency to slow the motion of the fluid and make it warmer as it move over the stretching sheet causing velocity U to decrease and temperature θ to increase. These behaviours are clearly illustrated in figs. 7 and 8.

The effect of variation of local Darcy Number on velocity and temperature profile is presented in figs. 9-10 respectively.It should be noted that large value of Da_x (more permeability) implies that the porous matrix structure becomes less and less prominent and the limit $Da_x \to \infty$ corresponds to the case of no porous medium present. Obvisouly a high porous medium exerts a less resistance to flow. This causes velocity U to increase as Da_x increases. This is clearly shown in fig. 9. However the presence of porous medium(smaller value of Da) has the tendency to enhance the fluid temperature θ due the increased fluid restriction resulting from the decreased porosity of the porous medium,asdepicted in fig. 10.

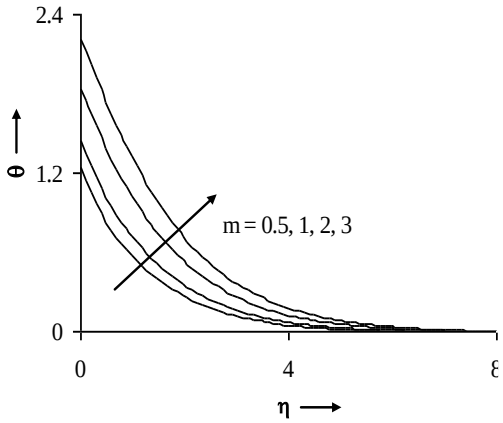

Fig. 4. Effects of velocity exponent m on temperature θ.

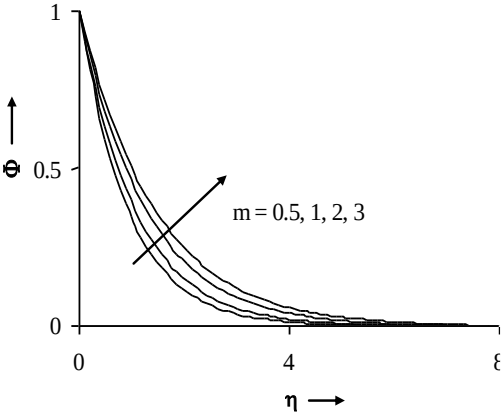

Fig. 5. Effects of velocity exponent m on concentration Φ.

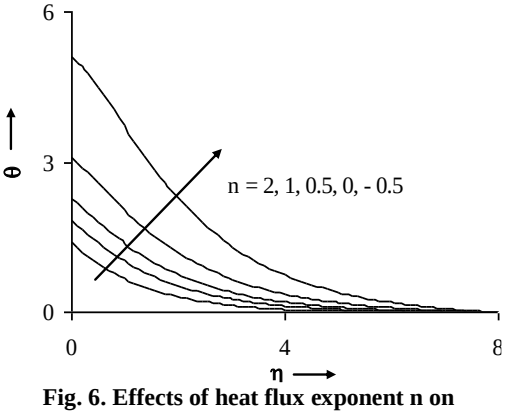

Fig. 6. Effects of heat flux exponent n on temperature.

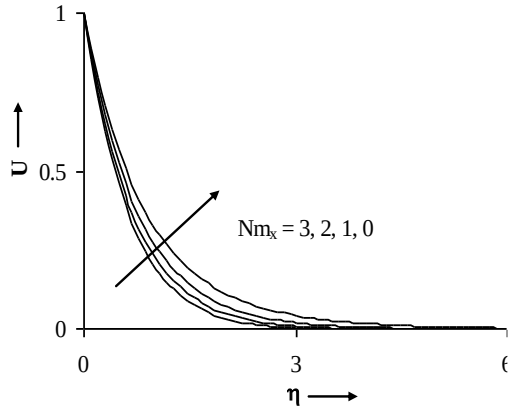

Fig. 7. Effects of Magnetic number Nm_x on velocity U.

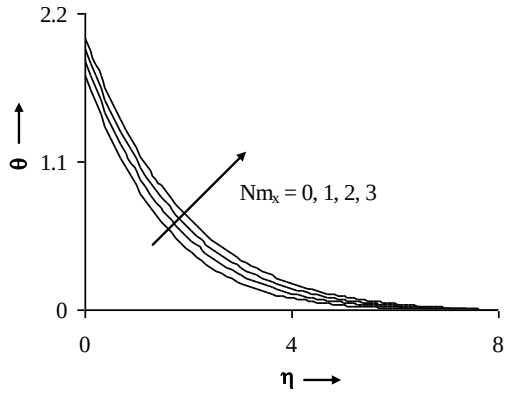

Fig. 8. Effects of Magnetic number Nm_x on temperature θ.

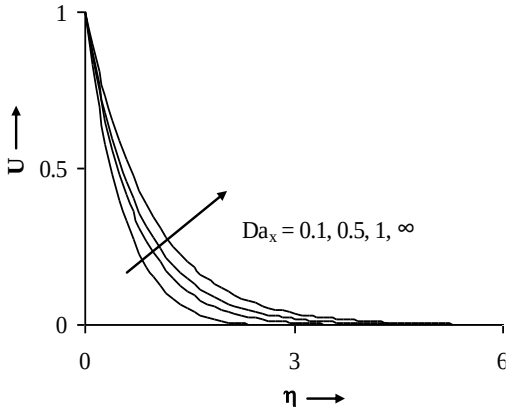

Fig. 9. Effects of Darcy number Da_x on velocity U

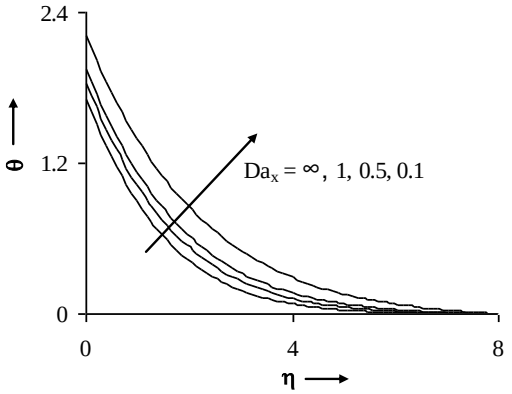

Fig. 10. Effects of Darcy number Da_x on temperature θ.

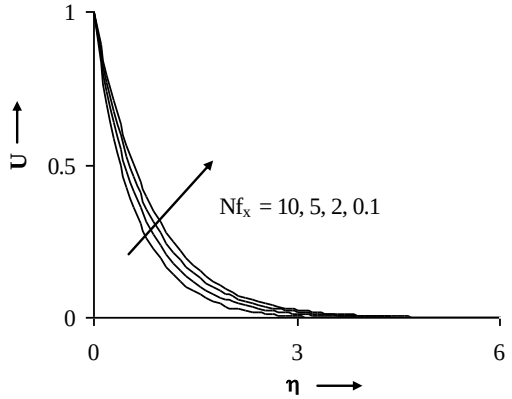

Fig. 11. Effects of Forchheimer number Nf_x on velocity U.

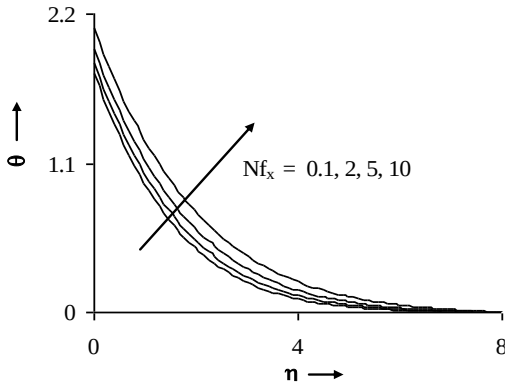

Fig. 12. Effects of Forchheimer number Nf_x on temperature θ.

The influence of local porous media inertial parameter, Nf_x,on the flow regime is demonstrated in Figs 11 and 12 for the reactive case.The porous medium inertial effects constitute resistance to the flow. Thus as the inertial parameter, Nf_x, increases, the resistance to the flow increases, causing the fluid flow to decelerate and the temperature to rise. Thus, Forchheimer drag has a positive influence on temperature but depresses fluid velocity.

Fig. 13 illustrates the effect of material parameter K on dimensionless temperature θ profile. It is observed that thermal boundary layer decreases when K increases. Besides this, one can notice that, temperature profile θ is a decreasing function of K i.e. temperature decreases as K increases. This fact is well in agreement with the findings of Hayat et. al.[13]

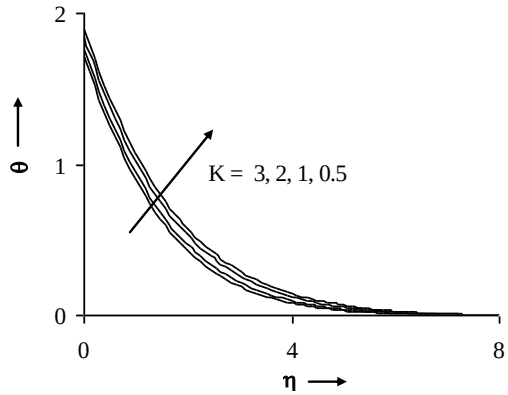

Fig. 13. Effects of Material parameter K on temperature θ.

The influence of Prandtl number Pr on temperature distribution can be seen in Fig. 14. The Prandtl number is a dimensionless number approximating the ratio of momentum diffusivity and thermal diffusivity. When *Pr* is small, it means that the heat diffuses very quickly compared to the velocity (momentum) resulting in a thicker boundary layer. Our computations also indicate that a rise in Pr substantially reduces the temperature in the micropolar-fluid-saturated porous regime as illustrated in Fig. 14.

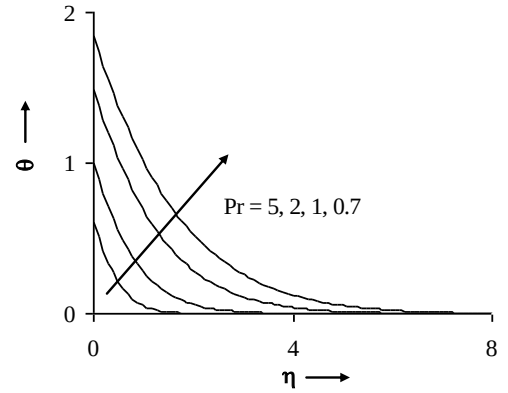

Fig. 14. Effects of Prandtl number Pr on temperature.

Fig. 15 plots the influence of chemical reaction parameter χ on the mass transfer function Φ. It is observed that as χ increases from 0 to 4, the concentration profile decreases noticeably. For the non-reactive case, $\chi = 0$, concentration profile shows approximately a linear decay from a maximum at the wall (vertical stretching surface i.e. at $\eta = 0$) to zero at the free stream (i.e. at $\eta = 8$), these end values being a direct result of the imposed boundary conditions. Asχ is increased, the profiles become more monotonic in nature; in particular the gradient of the profile becomes much steeper for $\chi = 4$ than for lower values of it. Thus chemical reaction parameter has a considerable influence on both magnitude and rate of species (mass) transfer function, since physically this corresponds to *faster* rates of reaction.

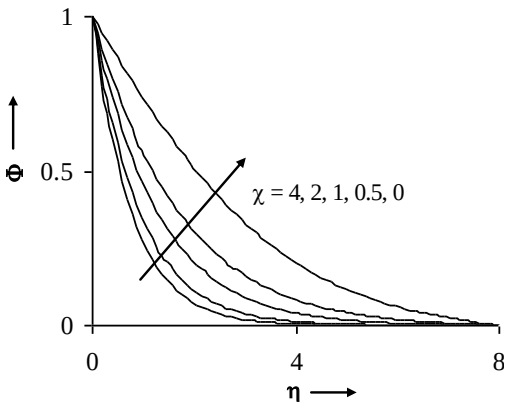

Fig. 15. Effects of Chemical reaction parameter χ on con.

The effect of Schmidt number, Sc, on the concentration Φ profiles is illustrated in fig. 16. Schmidt number is a dimensionless number defined as the ratio of momentum diffusivity (viscosity) and mass diffusivity. It physically relates the relative thickness of the hydrodynamic layer and mass-transfer boundary layer. Thus a lower value of Schmidt number indicate a thicker boundary layer as is illustrated in Figs 16.

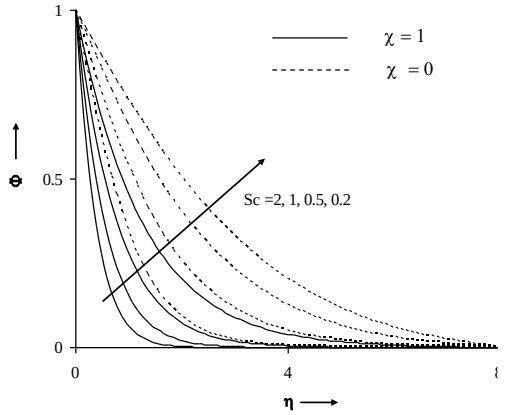

Fig. 16. Effects of Schmidt number Sc on concentration Φ, both in the presence andabsence of Chemical reaction parameter.

As Sc increases, for the *reactive flow case*, Φvalues are strongly reduced, since larger values of Sc are equivalent to a reduction in the chemical molecular diffusivity i.e. less diffusion therefore takes place by mass transport. Although the trends of influence of Sc on the concentration profiles for the non-reactive flow case are similar to that of the reactive flow case, the profiles are less decreased with a rise in Sc, in the absence of chemical reaction. For Sc = 0.2, there is almost a linear decay for the non-reactive case whereas it is considerably more parabolic for the reactive case, indicating lower values of Φ throughout the flow domain for the reactive case. We can therefore infer that in consistency with our earlier computations, chemical reaction decreases mass transfer markedly throughout the porous medium.

Table 3 indicates that as the value of K increases,

the skin friction parameter $-U'(0)$, and the wall couple stress, $-g'(0)$ both decreases. The numerical results also indicates that the micropolar fluid have a lower skin friction as compared to a Newtonian fluid under the same conditions.

Table 3 Effect of variation of material parameter K on $U'(0)$ and $g'(0)$

K	$U'(0)$	$g'(0)$
Newtonian case	1.54258	-
0.01	1.53785	0.513636
0.1	1.49879	0.511086
0.5	1.36883	0.460805
1.0	1.25867	0.400857
2.0	1.11755	0.318254
3.0	1.02766	0.266564
5.0	0.916288	0.266564

CONCLUSION

Flow, heat and mass transfer characteristics of a chemically reacting micropolar fluid flow over a non linear stretching sheet with variable heat flux and variable microinertia density in porous medium are analyzed in this paper.Our numerical computations indicates that:

- Heat transfer at the surface of the plate is enhanced with the increase in heat flux exponent n but decreases as Magnetic number increases.
- The velocity, temperature and concentration profiles boost with the increase in velocity exponent m. However, microrotation decreases at and near the wall with the rise in velocity exponent m.
- The velocity increases while temperature decreases with the rise in local Darcy number. The presence of porous medium with lower permeability (high solid material present) therefore can be used as a mechanism for decelerating flow velocities in industrial applications.
- Increasing Forchheimer number reduces velocity, but enhances temperature profiles throughout the flow regime.
- An increase in material parameter K leads to a decrease in skin friction as well as wall shear stress, or in other words micropolar fluid have lower skin friction as compared to a Newtonian fluid, a fact that can be of great relevance in automobile and many other industries. Also Increasing material parameter K leads to a decrease in dimensionless temperature θ profile.
- Prandtl number Pr considerably reduces the temperature function in the micropolar-fluid-saturated porous regime.
- Mass transfer function, Φ, substantially decreases with a rise in chemical reaction parameter (χ).
- Increasing Schmidt number reduces mass transfer function both in the reactive and non-reactive flow cases, although mass transfer function values are always higher for any Sc value in the non-reactive case ($\chi = 0$).

REFERENCES

Ahmadi, G. (1976). Self similar solution of incompressible micropolar boundary layer flow over a semi-infinite plate. *International Journal of Engineering Science 14, 639*.

Andersson H. I., O. R. Hansen and B. Holmedal (1994). Diffusion of a chemically reactive species from a stretching sheet. *Int. J. Heat Mass Transfer 37, 465*.

Beg O. A., R. Bhargava, S. Rawat, H. S. Takhar, Tasweer A. Beg and A. Study (2007). of Steady Buoyancy-Driven Dissipative Micropolar Free Convection Heat and Mass Transfer in a Darcian Porous Regime with Chemical Reaction. *Nonlinear Analysis: Modelling and Control 12, 157–180.*

Carragher P. and L. J. Crane (1982). Heat transfer on a continuous stretching sheet. *ZAMM 62, 564–565.*

Chakrabarti, A. Gupta and A. S. Hydromagnetic (1979). flow and heat transfer over a stretching sheet. *Q. Appl. Math. 37, 73.*

Chamkha J. A. (1997). MHD-free convection from a vertical plate embedded in a thermally stratified porous medium with Hall effects. Appl. *Math. Modelling 21, 603-609.*

Chiam T. C. (1998). Heat transfer in a fluid with variable thermal conductivity over a linearly stretching sheet. *Acta Mech. 129, 63–72.*

Cortell R., A. (2006). note on flow and heat transfer of a viscoelastic fluid over a stretching sheet. *Int. J. Non-Linear Mech. 41, 78–85*.

Eringen A. C. (1966). Theory of Micropolar Fluids. J. *Mathematics Mechanics 16, 1-18*.

Eringen A. C. (1972). Theory of thermomicropolar fluids. *J. Mathematical Analysis Applications 38, 480-496*.

Elbashbeshy, E. M. A (1998), Heat transfer over a stretching surface with variable surface heat flux, *J. Phys. D: Appl. Phys.311951-1954*.

Gorla, R. S. and R., Combined (1988). forced and free convection in micropolar boundary layer flow on a vertical flat plate *International Journal of Engineering Science 26(4), 385-391*.

Hayat T. Abbas Z and T. Javed (2008) Mixedconvection flow of a micropolar fluid over a non-linear stretching sheet. *Physics Letters A 372(5), 637-647.*

RawatS. and R. Bhargava (2009). Finite element study of natural convection heat and mass

transfer in a micropolar fluid-saturated porous regime with soret/dufour effects. *Int. J. of Appl. Math and Mech. 5(2), 58-71*.

Rawat S., R. Bhargava, S. Bég Rawat and R. Bhargava Hydromagnetic micropolar free convection heat and mass transfer in a darcy-forchheimer porous medium with thermophysical effects: finite element solutions . *Int. J. of Appl. Math and Mech, 6, 13, 72-93 (2010)*

Rawat S., R. Bhargava, S. Kapoor, O. A. Beg, Heat and Mass Transfer of a Chemically Reacting Micropolar Fluid Over a Linear Streaching Sheet in Darcy Forchheimer Porous Medium. International Journal of Computer Applications 44 , 6(2012), 40-51.

Rawat S., R Bhargava, S. Kapoor, O. A Beg, T. A Beg and R. Bansal (2014). Numerical Modeling of Two-Phase Hydromagnetic Flow and Heat Transfer in a Particle-Suspension through a non-Darcian Porous Channel. Journal of *Applied Fluid Mechanics 7, 2249-261*